Eur. Phys. J. Spec. Top. (2026) 235:8313–8319
https://doi.org/10.1140/epjs/s11734-026-02365-0

THE EUROPEAN PHYSICAL JOURNAL SPECIAL TOPICS

Check for updates

Regular Article

Effects of traumatic brain injury on interhemispheric and intrahemispheric EEG coherence in adolescents

G. A. Guyo[1,2,a], A. O. Trofimov[3], E. D. Volkova[3], A. N. Pavlov[1,2,4], and O. V. Semyachkina-Glushkovskaya[1]

[1] Saratov State University, Astrakhanskaya Str. 83, 410012 Saratov, Russia
[2] Regional Scientific and Educational Mathematical Center "Mathematics of Future Technologies", 410012 Saratov, Russia
[3] Privolzhsky Research Medical University, Minin and Pozharsky Sq. 10/1, 603950 Nizhny Novgorod, Russia
[4] Research Institute of Applied Artificial Intelligence and Digital Solution, Plekhanov Russian University of Economics, Stremyanny per. 36, 117997 Moscow, Russia

Received 22 March 2026 / Accepted 27 April 2026 / Published online 5 May 2026
© The Author(s), under exclusive licence to EDP Sciences, Springer-Verlag GmbH Germany, part of Springer Nature 2026

Abstract This paper examines how traumatic brain injury (TBI) affects the coherence of brain rhythms across different electrode pairs during the sleep–wake cycle. Stronger distinctions are observed for intrahemispheric compared to interhemispheric interactions. The direction of change in average coherence following TBI is found to depend on the location of the electrode pair, specifically whether the electrodes were positioned over anterior or posterior regions of the head. These findings suggest that a coherence-based approach is useful for monitoring recovery after brain injury.

1 Introduction

Electroencephalography (EEG) is a vital non-invasive tool in neurophysiology, routinely applied for the diagnosis of a wide spectrum of cerebral conditions [1, 2]. Its clinical utility is well-established in evaluating epilepsy, sleep architecture disorders, encephalopathies, and cognitive impairments [3–6]. Standard clinical practice involves the spectral analysis of key brain wave rhythms, with particular emphasis on their amplitude and dynamic interactions, to assess functional brain states and guide treatment decisions [7–9]. The importance of EEG is evident in the context of traumatic brain injury (TBI) [10–12]. Historically, it was the first ancillary method to objectively demonstrate post-traumatic cerebral dysfunction [10], often revealing abnormalities even when structural neuroimaging appeared normal. Today, continuous EEG monitoring has become an indispensable tool in neurocritical care, employed not only for the early detection and prediction of post-traumatic epilepsy [13] but also as a valuable prognostic marker for long-term neurological outcomes and recovery trajectories in TBI patients [14, 15]. However, emerging evidence suggests that traditional EEG analysis, which primarily focuses on dominant rhythms, may lack the sensitivity required to fully characterize the complex and dynamic alterations in brain states following TBI [16]. This limitation underscores the need for more advanced analytical techniques, such as those based on network approaches, particularly on the application of functional brain network analysis [17–22].

The electroencephalographic manifestations of TBI are highly heterogeneous and depend critically on the severity of the injury. While EEG-based detection of TBI-related abnormalities holds significant promise as a powerful neurodiagnostic modality, its current clinical utility remains limited, particularly in cases of mild TBI, which account for approximately 90% of all TBI cases [23]. To date, no specific or clearly defined EEG signature has been established for mild TBI, rendering conventional EEG analysis insufficient for reliable detection in this prevalent patient population [10, 24]. Consequently, the development of sensitive methods for EEG analysis in TBI has emerged as a challenge in modern medicine. Our preliminary investigations, based on available EEG databases from TBI patients, have revealed notable alterations in sleep architecture related to daytime recordings. In adult patients (particularly those in older age groups), a complete sleep cycle encompassing deep sleep stages is rarely observed. Instead, sleep is typically restricted to the lighter stages N1 and N2. These findings are consistent with reports from other research groups, who have similarly documented pronounced insomnia and sleep fragmentation in adults following TBI. Intriguingly, our observations in younger TBI patients revealed a markedly different

[a] e-mail: guyo199814@gmail.com (corresponding author)

pattern. In contrast to adults, adolescent patients exhibited preserved sleep architecture, including the presence of all sleep stages and, notably, deep sleep.

This age-dependent discrepancy in sleep continuity following TBI motivated the present study. In this paper, we therefore focus on investigating the effects of TBI on the coherence of EEG rhythms in adolescents across different stages of the sleep–wake cycle. Furthermore, we compare these patterns of rhythm coherence with those observed in age-matched relatively healthy controls, aiming to identify potential biomarkers of TBI-related brain dysfunction that may be specific to the developing brain. As the primary methodological approach, this study employs the estimation of averaged coherence [25] across the frequency bands corresponding to the principal EEG rhythms, encompassing both interhemispheric and intrahemispheric connections. Coherence analysis provides a robust measure of functional connectivity, quantifying the degree of synchrony between neuronal populations in different cortical regions. Previous research has demonstrated that traumatic brain injury induces significant alterations in EEG coherence patterns during cognitive tasks [26].

This paper is organized into four sections. Section 2 describes the experimental setup and the EEG data processing techniques. Section 3 presents the results, highlighting differences in brain wave coherence between TBI patients and healthy controls across different brain regions. Section 4 concludes with a summary of the main findings.

2 Materials and methods

2.1 Subjects and experimental data

Protocol of experiments was approved by the Local Ethics Committee of the Clinical pediatrician hospital in Nizhny Novgorod. Written informed consent was obtained from the parents of all participants prior to enrollment. Demographic and clinical data, including age, sex, injury severity assessed by the Glasgow Coma Scale (GCS), and functional outcome measured by the Glasgow Outcome Scale Extended (GOS-E), were recorded for all participants. The inclusion criteria were as follows: (1) moderate TBI, defined as a GCS score of 9–12 on admission and 13–15 by the 10th day of treatment; (2) age between 14 and 18 years; and (3) absence of MRI and/or CT evidence of parenchymal hemorrhagic foci. The exclusion criteria comprised: (1) age under 14 or over 18 years; (2) concomitant extracranial injuries (Injury Severity Score > 9); (3) a history of TBI, epilepsy, cerebral palsy, or any other chronic neurological disorders; (4) mild or severe TBI (GCS < 9 or > 13 on admission); (5) MRI and/or CT signs of intracranial parenchymal hemorrhage; and (6) absence of electroencephalographic signs of deep sleep [27, 28].

Multichannel EEG recordings were obtained using a Neuron-Spectr.NET system (v. 2.0.27.1, Neurosoft, Russia) between the 3rd and 5th days after hospital admission. All recordings were performed in a dedicated EEG suite at the Department of Neurophysiology during daytime hours, with each session lasting 2–3 h and with a preliminary sleep deprivation. Two groups of participants were included in the analysis: (i) a control group of healthy adolescents (median age 15.9 years; $n = 12$) and (ii) a group of adolescents with moderate TBI (median age 16.2 years; $n = 12$). In all participants, the EEG recordings captured sleep architecture encompassing the lightest stage (N1), light sleep (N2), and deep sleep (N3). The signals were digitized at a sampling rate of 500 Hz. For subsequent analysis, artifact-free segments of at least 3 min duration were selected for each sleep stage.

The study employed EEG recordings from electrodes placed at F3, F4, C3, C4, P3, P4, O1, and O2. To assess intrahemispheric connectivity, functional coupling was analyzed within the left (F3–C3, C3–P3, P3–O1) and right (F4–C4, C4–P4, P4–O2) hemispheres. Interhemispheric interactions were evaluated through symmetrical fronto-frontal (F3-F4), centro-central (C3–C4), parieto-parietal (P3–P4), and occipito-occipital (O1–O2) electrode pairs.

2.2 Coherence analysis

To assess functional connectivity, mean coherence values (γ) were computed for five frequency bands: delta (0.5–4 Hz), theta (4–8 Hz), alpha (8–12 Hz), sigma (12–16 Hz), and beta (16–20 Hz). Coherence estimates were derived using a standard spectral analysis approach [25], wherein cross-spectral densities were calculated for each pair of signals from different electrode pairs. The resulting coherence spectra were then averaged across the frequencies within each band of interest, providing a robust measure of synchronization between neural oscillatory activities in the respective frequency ranges.

3 Results and discussion

The analysis of average coherence was initially conducted for each rhythm separately, considering intrahemispheric channels within the left and right hemispheres, as well as interhemispheric connections. Some of the results obtained

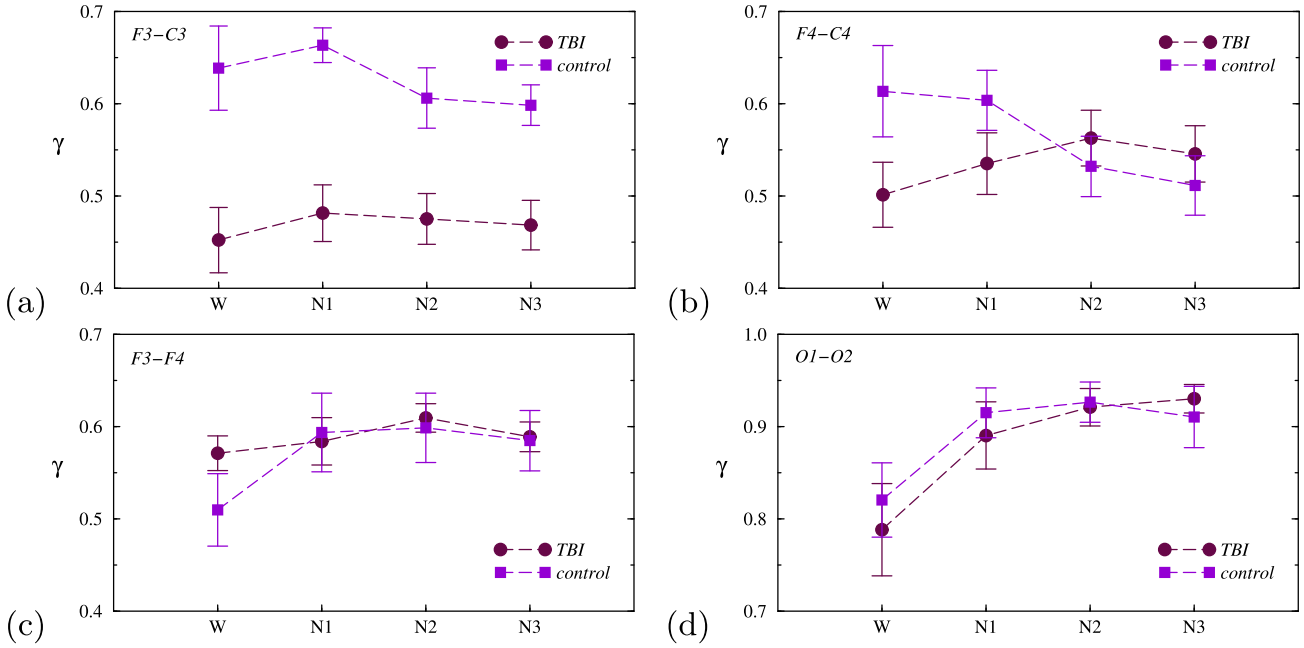


Fig. 1 Typical examples of changes in average coherence (for the delta rhythm) following TBI for several intrahemispheric interactions: the F3–C3 (**a**) and F4–C4 (**b**) electrode pairs, as well as interhemispheric interactions: the F3–F4 (**c**) and O1–O2 (**d**) electrode pairs

for the delta rhythm are shown in Fig. 1. As illustrated in the figure, various patterns of changes in coherence were observed at TBI across different stages of the sleep–wake cycle, compared to the control group. These include a pronounced decrease in coherence (γ) throughout all stages (pair F3–C3, Fig. 1a); a decrease observed only in certain stages (wakefulness, N1), followed by a slight increase above the control group's coherence level (pair F4–C4, Fig. 1b); subtle changes during sleep (pair F3–F4, Fig. 1c); and only minor variations across all stages of the sleep-wake cycle (pair O1–O2, Fig. 1d). These findings highlight the diversity of changes in the coherence dynamics of EEG rhythms across different channel pairs. Similar patterns were observed not only for the delta rhythm but also for other EEG rhythms. Given the relatively small sample size of the experiments, which may influence the results and the conclusions of the study, further analysis was performed by averaging across all five selected rhythms in order to obtain a more objective and generalized view of the observed effects.

Figure 2 presents the results of estimating the quantity

$$| \Delta\gamma | = \sum_{i=1}^{5} | \gamma^i_{TBI} - \gamma^i_{control} |, \tag{1}$$

where i denotes the rhythm index. The estimations were performed separately for each sleep stage and are presented as mean values ± standard error of the mean. In this case, the focus was not on the qualitative nature of coherence changes (i.e., whether it increased or decreased), but rather on the magnitude of differences between the normal and pathological conditions. According to the obtained results, the most pronounced changes were observed in

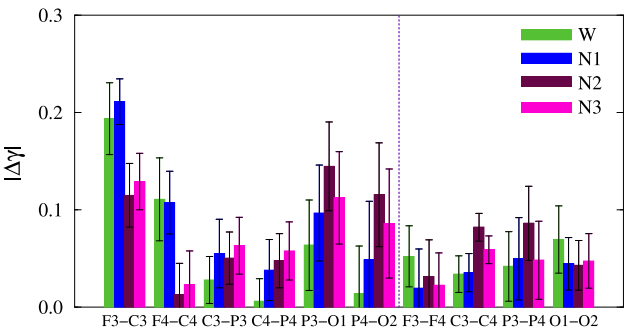


Fig. 2 The measure (1) estimated for all analyzed electrode pairs and all stages of the sleep–wake cycle. Here and throughout, the dashed line separates cases of intrahemispheric and interhemispheric interactions

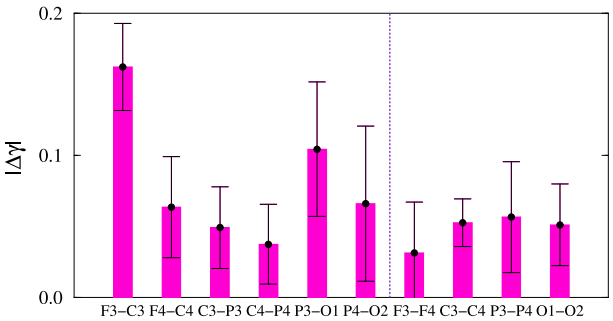


Fig. 3 The measure (1) estimated for all analyzed electrode pairs after averaging across stages of the sleep–wake cycle

the left hemisphere (channel pairs F3–C3, P3–O1). For these channel pairs, significant differences were found in every stage of the sleep–wake cycle. Less pronounced differences (significant for two stages of the cycle) were also observed in channel pairs within the right hemisphere (F4–C4 for stages W and N1; P4–O2 for stages N2 and N3). For other channel pairs, differences may be significant for all or some stages of the sleep–wake cycle; however, in terms of absolute changes of the measure (1), these differences were less prominent compared to those mentioned above. Thus, the performed estimates reveal a certain asymmetry—more pronounced changes in the left hemisphere compared to the right, as well as stronger alterations in intrahemispheric connectivity following TBI compared to interhemispheric connectivity.

Figure 3 illustrates the results of averaging $|\Delta\gamma|$ across all sleep stages to confirm the overall pattern of changes. In descending order of this measure, the channel pairs are ranked as follows: F3–C3 and P3–O1 (left hemisphere), followed by P4–O2 and F4–C4 (right hemisphere), and only then the interhemispheric channel pairs P3–P4, C3–C4, and O1–O2.

It should be noted that the observed changes are not limited to a single specific rhythm; rather, they are manifested to a greater or lesser extent across all analyzed frequency bands, as summarized in Table 1.

Next, a more detailed analysis is conducted, taking into account the sign of the changes in $\Delta\gamma$, estimated as

$$\Delta\gamma = \sum_{i=1}^{5} (\gamma^i_{TBI} - \gamma^i_{control}). \tag{2}$$

It should be noted that this approach correlates with Eq. (1) in terms of the absolute values of the computed measure, provided that the changes in average coherence are consistent across all sleep stages. If, for example, alternating patterns occur (as shown in Fig. 1b), the computed values will be substantially smaller than in the first case.

Figure 4 illustrates the changes in average coherence following TBI, taking their signs into account. The most pronounced changes are again observed in the left-hemisphere channel pairs F3–C3 and P3–O1, but now they exhibit opposite trends: in the first pair, measure (2) decreases after TBI, while in the second, it increases. A

Table 1 Values of $|\Delta\gamma|$ computed separately within the frequency band of each EEG rhythm

Channel pair	Coherence measure				
	Delta	Theta	Alpha	Sigma	Beta
F3–C3	0.157	0.148	0.182	0.154	0.169
F4–C4	0.061	0.048	0.061	0.078	0.068
C3–P3	0.043	0.027	0.037	0.084	0.054
C4–P4	0.044	0.030	0.025	0.037	0.051
P3–O1	0.141	0.112	0.062	0.097	0.110
P4–O2	0.071	0.063	0.043	0.074	0.080
F3–F4	0.021	0.023	0.040	0.043	0.029
C3–C4	0.046	0.071	0.065	0.047	0.035
P3–P4	0.116	0.070	0.023	0.043	0.030
O1–O2	0.020	0.039	0.058	0.069	0.070

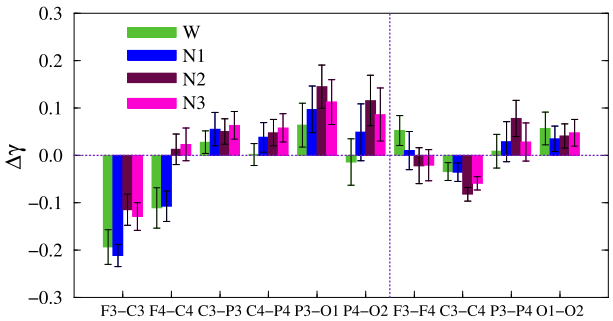


Fig. 4 The measure (2) computed for all analyzed electrode pairs and all stages of the sleep–wake cycle

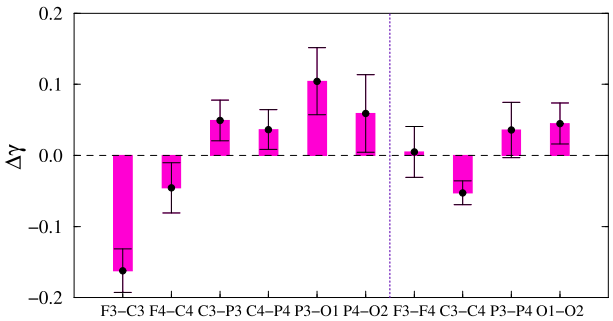


Fig. 5 The measure (2) computed for all analyzed electrode pairs after averaging across stages of the sleep–wake cycle

relatively strong decrease in average coherence is observed for the F4–C4 pair in two stages (W, N1), accompanied by a corresponding increase for the P4–O2 pair (N2, N3). These may be accompanied by a sign reversal of $\Delta\gamma$ in other stages for some individual subjects, but overall, this effect is not statistically significant across the group. For interhemispheric interactions, the changes are less pronounced, and the sign-reversal effect is also not significant at the group level, although it is observed in some individual cases.

The differences averaged across all sleep stages are presented in Fig. 5, which confirms the previous findings and allows us to highlight the following features. With the exception of the relatively small changes observed in the F3–F4 channel pair, in the anterior regions of the head (channel pairs F3–C3, F4–C4, C3–C4), TBI in adolescents predominantly leads to a decrease in average coherence of key EEG rhythms. In contrast, in the posterior regions (channel pairs C3–P3, C4–P4, P3–O1, P4–O2, P3–P4, O1–O2), average coherence increases. Thus, changes in coherence are determined not only by the type of connectivity (intrahemispheric vs. interhemispheric, although the former shows more pronounced changes) but also by the location of the electrode pairs.

4 Conclusion

This study investigated the effects of traumatic brain injury on the coherence of EEG rhythms, examining distinctions across various electrode pairs and stages of the sleep–wake cycle. The findings reveal a distinct pattern: for certain electrode pairs, significant differences between adolescents with TBI and healthy controls were consistently observed across all stages of the cycle. In contrast, for other electrode pairs, statistically significant changes emerged only during specific stages, suggesting that the impact of TBI on neural connectivity is not uniform across either brain regions or functional states. Notably, pronounced differences in average coherence were identified for intrahemispheric interactions, particularly within the left hemisphere, when compared to interhemispheric interactions. This lateralized effect may reflect the differential vulnerability of neural networks following injury. Furthermore, the directionality of coherence changes (whether coherence increased or decreased in adolescents with TBI) was associated with the spatial location of the electrode pair. Specifically, the nature of these changes differed depending on whether the electrodes were placed over anterior versus posterior regions of the head, pointing to region-specific alterations in functional connectivity. Taken together, these results underscore the potential of coherence-based EEG analysis as a sensitive and non-invasive tool for assessing functional recovery after brain injury. By capturing both the spatial and state-dependent dynamics of neural communication, this approach may offer valuable insights for clinical monitoring and rehabilitation planning.

Acknowledgements This work was supported by the Russian Science Foundation, Russia, grant no. 23-71-30010.

Author contribution statement

Authors contributions are as followed: conceptualization, A.N.P. and O.V.S.-G.; methodology, A.N.P. and O.V.S.-G.; data curation, A.O.T. and E.D.V.; software, G.A.G.; formal analysis, G.A.G.; investigation, G.A.G. and A.N.P.; writing—original draft preparation, G.A.G. and A.N.P.; writing—review and editing, O.V.S.-G.; visualization, G.A.G.; supervision, A.N.P. and O.V.S.-G. All authors have read and agreed to the published version of the manuscript.

Data availability The datasets generated during and/or analyzed during the current study are available from the corresponding author on reasonable request.

Declarations

Conflict of interest The authors have no conflict of interest to declare that are relevant to the content of this article.

References

1. G. Buzsáki, *Rhythms of the Brain* (Oxford University Press, Oxford, 2006)
2. E. Niedermeyer, F. Lopes da Silva, *Electroencephalography: Basic Principles, Clinical Applications and Related Fields*, 5th edn. (Lippinkot Williams & Wilkins, Philadelphia, 2005)
3. M.M. Siddiqui, R. Jain, M.S. Kidwai, M.Z. Khan, Recording of EEG signals and role in diagnosis of sleep disorder. Biomed. Pharmacol. J. **15**, 1421–1426 (2022)
4. D. Weber, EEG in Epilepsy. Continuum (Minneap Minn) **31**, 38–60 (2025)
5. V. Papaliagkas, The role of quantitative EEG in the diagnosis of Alzheimer's disease. Diagnostics **15**, 1965 (2025)
6. Z. Huang, Y. Yang, Y. Ma, Q. Dong, J. Su, H. Shi, S. Zhang, L. Hu, EEG detection and recognition model for epilepsy based on dual attention mechanism. Sci. Rep. **15**, 9404 (2025)
7. W.H. Miltner, C. Braun, M. Arnold, H. Witte, E. Taub, Coherence of gamma-band EEG activity as a basis for associative learning. Nature **397**, 434–436 (1999)
8. W. Klimesch, EEG alpha and theta oscillations reflect cognitive and memory performance: a review and analysis. Brain Res. Rev. **29**, 169–195 (1999)
9. K. Schindler, H. Leung, C.E. Elger, K. Lehnertz, Assessing seizure dynamics by analysing the correlation structure of multichannel intracranial EEG. Brain **130**, 65–77 (2007)
10. A. Kadri, N. Apriani, Electroencephalography findings in traumatic brain injury. Open Neurol. J. **16**, e1874205X2206100 (2022)
11. K. Politi, P.L. Weiss, K. Givony, E. Zion Golumbic, Utility of electroencephalograms for enhancing clinical care and rehabilitation of children with acquired brain injury. Int. J. Environ. Res. Public Health **21**, 1466 (2024)
12. F. Manzari, P. Ghaderyan, Insights into computer-aided EEG signal processing for traumatic brain injury assessment: a review. Measurement **251**, 117279 (2025)
13. J. Pyrzowski, M. Kalas, M. Mazurkiewicz-Beldzińska, M. Siemiński, EEG biomarkers for the prediction of post-traumatic epilepsy—a systematic review of an emerging field. Seizure **119**, 71–77 (2024)
14. H.J. van der Horn, J.M. Spikman, B. Jacobs, J. van der Naalt, Postconcussive complaints, anxiety, and depression related to vocational outcome in minor to severe traumatic brain injury. Arch. Phys. Med. Rehabil. **94**, 867–874 (2013)
15. P.K.B. Tewarie, T.M.J. Beernink, C.J. Eertman-Meyer, A.D. Cornet, A. Beishuizen, M.J.A.M. van Putten, M.C. Tjepkema-Cloostermans, Early EEG monitoring predicts clinical outcome in patients with moderate to severe traumatic brain injury. Neuroimage Clin. **37**, 103350 (2023)
16. A. Lin, K.K.L. Liu, R.P. Bartsch, P.C. Ivanov, Dynamic network interactions among distinct brain rhythms as a hallmark of physiologic state and function. Commun. Biol. **3**, 197 (2020)
17. A.E. Hramov, N.S. Frolov, V.A. Maksimenko, S.A. Kurkin, V.B. Kazantsev, A.N. Pisarchik, Functional networks of the brain: from connectivity restoration to dynamic integration. Phys. Usp. **64**, 584 (2021)
18. E.N. Pitsik, V.A. Maximenko, S.A. Kurkin, A.P. Sergeev, D. Stoyanov, R. Paunova, S. Kandilarova, D. Simeonova, A.E. Hramov, The topology of fMRI-based networks defines the performance of a graph neural network for the classification of patients with major depressive disorder. Chaos Solitons Fract. **167**, 113041 (2023)
19. V.S. Khorev, S.A. Kurkin, G. Zlateva, R. Paunova, S. Kandilarova, M. Maes, D. Stoyanov, A.E. Hramov, Disruptions in segregation mechanisms in fMRI-based brain functional network predict the major depressive disorder condition. Chaos Solitons Fract. **188**, 115566 (2024)
20. S.A. Kurkin, L.A. Mayorova, V.S. Khorev, E.N. Pitsik, M.L. Radutnaya, E.L. Bondar, A.E. Hramov, Multiscale fMRI analysis reveals hierarchical network disruptions underlying disorders of consciousness. Chaos Solitons Fract. **200**, 117008 (2025)
21. S.A. Kurkin, A.N. Pisarchik, L.A. Mayorova, A.E. Hramov, Evolution of methods for assessing fMRI-based functional networks: from classical pairwise connectivity to higher-order interactions. Phys. Rep. **1174**, 1–66 (2026)

22. D. Stoyanov, V. Khorev, R. Paunova, S. Kandilarova, D. Simeonova, A. Badarin, A. Hramov, S. Kurkin, Resting-state functional connectivity impairment in patients with major depressive episode. Int. J. Environ. Res. Public Health **19**(21), 14045 (2022)
23. A.T. Alouani, T. Elfouly, Traumatic brain injury (TBI) detection: past, present, and future. Biomedicines **10**, 2472 (2022)
24. M.J. Aminoff, Electroencephalography: general principle and clinical applications, in *Aminoff's Electrodiagnosis in Clinical Neurology*, 6th edn. (Elsevier Saunders, San Francisco, 2016), pp.37–84
25. J.S. Bendat, A.G. Piersol, *Random Data: Analysis and Measurement Procedures* (Wiley, Hoboken, 2011)
26. I. Méndez-Balbuena, B.L. Betancourt-Navarrete, A.C. Hermosillo-Abundis, A. Flores, L.F. Rebolledo-Herrera, R. Lemuz-López, N. Huidobro, R. Meza-Andrade, H.J. Pelayo-González, M.D.R. Bonilla-Sánchez, V.A. López-Cortes, M.A. García-Flores, Weighted coherence analysis as a window into the neurophysiological effects of traumatic brain injury. Bioengineering **11**, 1187 (2024)
27. G.A. Guyo, A.O. Trofimov, E.D. Volkova, O.N. Pavlova, A.N. Pavlov, O.V. Semyachkina-Glushkovskaya, Phenomenon of adjustment of brain rhythm coordination in healthy adolescents and with traumatic brain injury: an important marker of post-traumatic brain restoration. Chaos **35**, 103130 (2025)
28. V.V. Adushkina, A.O. Trofimov, E.D. Volkova, O.N. Pavlova, G.A. Guyo, A.N. Pavlov, Cooperative dynamics of EEG rhythms in adolescents with traumatic brain injuries. Eur. Phys. J. Spec. Top. (2026). https://doi.org/10.1140/epjs/s11734-026-02160-x

Springer Nature or its licensor (e.g. a society or other partner) holds exclusive rights to this article under a publishing agreement with the author(s) or other rightsholder(s); author self-archiving of the accepted manuscript version of this article is solely governed by the terms of such publishing agreement and applicable law.